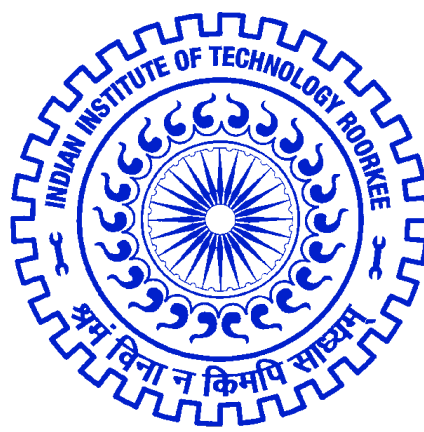

Mechanical Behavior of Porous Shape Memory Alloy Composites

*A thesis submitted in fulfilment of the requirements
for the degree of Master of Technology*

by

Dinesh Chandra Pant



DEPARTMENT OF MECHANICAL ENGINEERING
INDIAN INSTITUTE OF TECHNOLOGY ROORKEE

November 2016

Condidate's Declaration

I hereby declare that the work carried out in the dissertation titled “Mechanical Behavior of Porous Shape Memory Alloy Composites” is presented on behalf of partial fulfilment of the requirement for the award of the degree of Master of Technology in the specialization of CAD CAM & ROBOTICS submitted to the department of Mechanical & Industrial Engineering, Indian Institute of Technology Roorkee under the supervision and guidance of Dr. Siladitya Pal, Assistant Professor MIED IIT Roorkee.

I have not submitted the matter embodied in this report for the award of any other degree or diploma.

Date:

November 2016

Dinesh Chandra Pant

Certificate

This is to certify that the thesis entitled “Mechanical Behavior of Porous Shape Memory Alloy Composites” is submitted by Dinesh Chandra Pant (Enrolment No.15538003) in the partial fulfilment of the requirements for the award of Master of Technology degree in CAD, CAM & ROBOTICS (MIED) specialisation at Indian Institute of Technology, Roorkee under my supervision and guidance

Dr. Siladitya Pal

November 2016

Professor

Department of Mechanicall Engineering
Indian Institute of Technology Roorkee

Abstract

Porous Shape Memory Alloys (SMA) are derivatives of SMAs which can offer better properties such as light weight, high energy absorption, damping capacity and good biocompatibility. Recently, several experiments have been carried out to investigate the effect of porosity on mechanical behavior of porous SMA. Although, major studies focused on quasi-static response of porous SMA, there is an impetus towards understanding its high strain rate behavior for its potential applications as energy absorbing materials. However, high strain rate behavior of porous SMA remain unclear so far. The mechanical behavior of porous SMA is investigated in the present study for various strain rate regimes. A non-linear finite element framework is adopted to solve the governing equations and an explicit time integration algorithm is employed. Forward Euler algorithm is used to solve the non-linear constitutive behavior. A parametric study is performed systematically considering various shapes, sizes and distribution of pores in the SMA matrix at different strain rates.

Acknowledgements

I wish to express my deep sense of gratitude and sincere thanks to my guide **Dr. Siladitya Pal** (assistant professor of Mechanical and Industrial Engineering department, IIT Roorkee) for being helpful and a great source of inspiration. I would like to thank him for providing me an opportunity to work on this excellent and innovative field of research. I wish to thank him for his constant guidance and suggestions without which I could not have progressed this dissertation work. I would also like to thank all the teaching and non-teaching staff members of the department who have contributed directly or indirectly for creating a conducive environment.

Date:

November 2016

Dinesh Chandra Pant

Contents

Condidate's Declaration	i
Certificate	ii
Abstract	iii
Acknowledgements	iv
Contents	v
List of Figures	vii
List of Tables	viii
1 Introduction	1
1.1 Introduction	1
1.2 Shape memory alloy materials	2
1.2.1 Bulk shape memory alloy	2
1.2.2 Application of Shape memory alloy	3
1.3 Porous Shape Memory Alloy	4
2 Literature Review	6
2.1 Literature	6
2.2 Technical Challenges	8
2.3 Research objectives	9
2.4 Scope of present study and progress report organization	9
3 Formulation of Computational Framework	10
3.1 Governing equations	10
3.2 Explicit finite element formulation	12
3.2.1 Variational formulation	12
3.2.2 Finite element model	12

3.2.3	Explicit Time Integration scheme	13
3.3	SMA Constitutive Model	14
3.3.1	Evolution of Internal Variables	15
4	High Strain Behavior of Porous Shape Memory Alloy	18
4.1	Introduction	18
4.2	Problem definition	19
4.3	Results and discussions	20
4.3.1	Variation of material response for different strain rates at fixed porosity	20
4.3.2	Stress-strain response of material with varying porosity at fixed strain rate	22
4.3.3	Effect of strain rate on strength ratio of porous SMA	24
5	Conclusion and Future Plan	25
5.1	Findings of present work	25
5.2	Future work Plan	26

List of Figures

1.1	Shape memory effect and Pesudoelastic behavior of SMA[9]	2
1.2	Boeing's variable geometry chevron[42]	3
1.3	Self expanding stents[9]	3
1.4	SMA Shok Absorber	4
1.5	SMA application in Golf-stick	4
1.6	Tennis Racket of SMA strip	4
1.7	Sports shoes of SMA	4
1.8	Alterable stiffness medical implant Ronny Pfeifera [70]	5
1.9	Porous SMA unit cell	5
3.1	Schematic of generic problem in solid mechanics	11
4.1	Homogeneous strain loading condition	19
4.2	Quasi-static and Dynamic behavior of porous SMA	21
4.3	stress-strain behavior of bulk SMA	22
4.4	stress-strain behavior of 13.08% porosity level	22
4.5	stress-strain behavior of 29.43% porosity level	22
4.6	Energy absorption charactersitics of Porous SMA for different strain rate	22
4.7	Stress strain rate behavior at 10^3 strain rate	23
4.8	Stress strain rate behavior at 10^4 strain rate	23
4.9	Stress strain rate behavior at 10^5 strain rate	23
4.10	Energy absorption charactersitics of Porous SMA for different porosity level	23
4.11	Variation of strength ratio with strain rate	24

List of Tables

For/Dedicated to/To my...

Chapter 1

Introduction

1.1 Introduction

Shape memory alloy are the novel materials, which was first discovered by Olander [63]. The term 'Shape Memory Alloy' was first introduced by Vernon and Vernon [87] but no focus was given until [88, 44] revealed extra-ordinary characteristic of remmemberring its original shape. Shape memory alloy is a special class of material which is capable of undergoing a reversible solid to solid phase transformation under thermal/mechanical loading which may result in large deformation and inelastic stress of 1-8%. SMA consists of two phases usually at high temperature and low stress value it has higher symmetry austanite phase but at low temperature and high stress value it has lower symmetry phase called as martensitis phase. It has two smart behaviour resulting from transformation i.e. Shape memory effect and pseudoelsticity Since the discovery of Shape memory effect and pseudoelastic behaviour the demand for SMAs in different areas of engineering and science field has arises such as: Automotive [23, 83, 21, 44], Aerospace [89, 40, 57], Strcultural applications, Vibration dampers Casciati et al. [22], Energy absorption Zhao et al. [92], Robotics [69, 77, 81, 54] and Biomedical [17, 66, 79, 53].For detailed application of SMA interesting readers are suggested to follow a review article on SMA applications by Mohd et al. [58]. Due to these nice behaviour people thought about utilising such key behaviour and that is done in two approaches-(1) To develop new material and alloys (2) creation of hybrid material that combines the characteristics of existing material, following the first approach researcher are developing new material such as magnetic shape memory alloy, high temperature shape memory alloy. While in second approach various porous shape memory composites are developed, there are several application of such composites

in present e.g.-SMA wires, SMA beams, structure. Following are some different type of shape memory alloy materials.

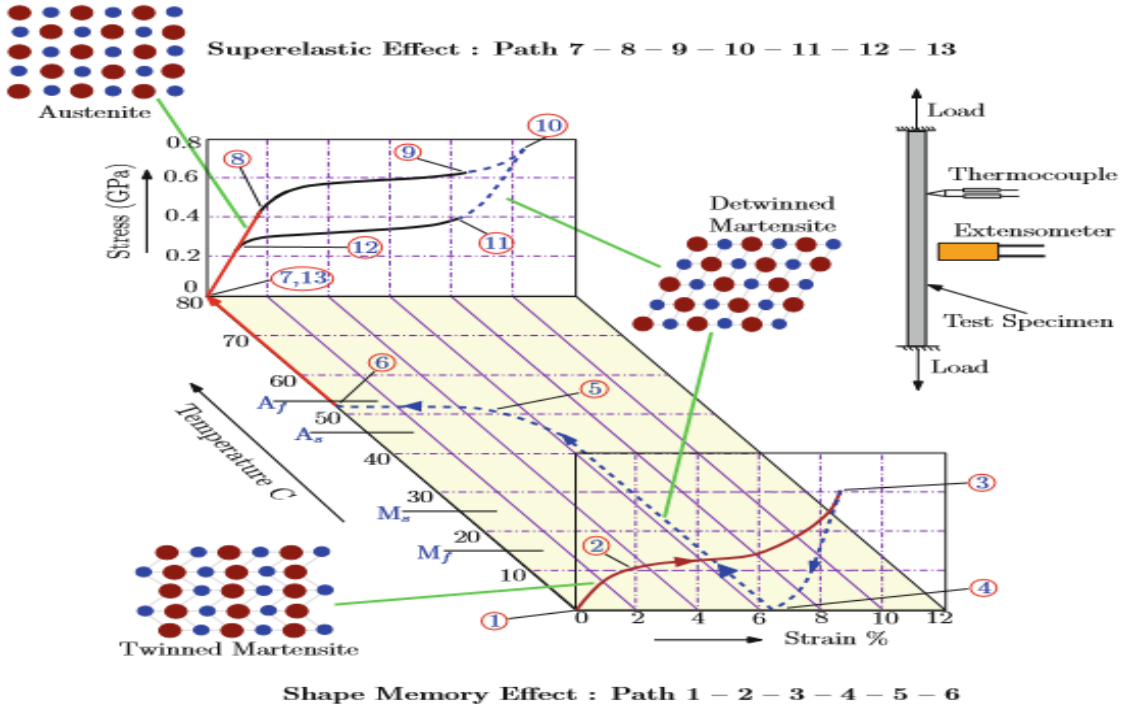


FIGURE 1.1: Shape memory effect and Pesudoelastic behavior of SMA[9]

1.2 Shape memory alloy materials

1.2.1 Bulk shape memory alloy

Ti—Ni system alloys During the last three decades, the binary Ti—Ni alloys have been intensively investigated and nowadays are the most important commercial SMAs because of their exclusive shape-memory performance, good processibility, and excellent mechanical properties. In addition, the alloys have very good corrosion resistance and biocompatibility, which enable them to be widely used in the biomedical field. Because the Ti—Ni alloys can be readily fabricated into various forms or sizes, it is technically feasible to make them an active element in various composites. In particular, Ti—Ni thin films, fibres, particles and porous bulks have been successfully fabricated in recent years, and these materials, either in the monolithic form or in combination with other materials, have exhibited some exciting application potentials in microelectromechanical systems, medical implants, intelligent materials and structural system.

Copper-based alloys. Compared to Ni-Ti alloys Copper based alloys has some advantages such as reduced cost and simple procedure of fabrication. However these alloys have limited application because of low ductility which results from high elastic anisotropy and coarse grain size. Copper based alloys may be a good candidate for high temperature application due to their high thermal stability if poor processibility can be improved. Recently several attention has been given to improve processibility of these alloys as a result few quaternary and pentonic alloys have been developed whose martensite start temperature is above 429K.

Iron-based alloys Because price is major concern of any application so iron shape memory alloys have attracted considerable attention from recent years due to easy availability of iron. Along with thermal and mechanical stimuli these type of alloys are sensitive to magnetic fields that is why termed as Ferromagnetic shape memory alloys.

1.2.2 Application of Shape memory alloy

Due to unique behavior of SMA wide range of application has been found from past two decades although it was investigated in 1960s. Its application includes energy absorbing devices, vibration dampers, aerospace, automobile and biomedical fields.

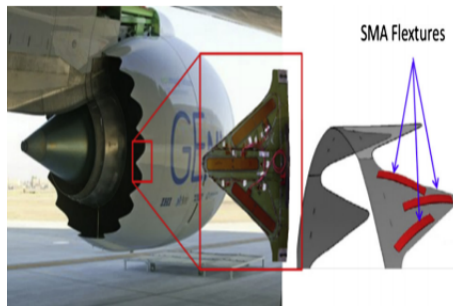


FIGURE 1.2: Boeing's variable geometry chevron[42]

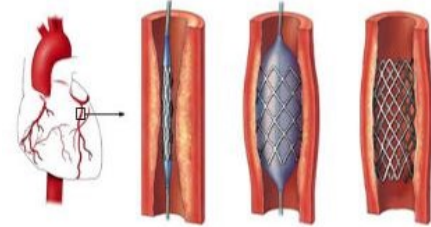


FIGURE 1.3: Self expanding stents[9]

Figure 1.2 shows a chevron which is used in Boeing aeroplane, the objective of this is to reduce noise and increase cruising speed of the aeroplane. Figure 1.3 shows a self-expanding stent, which can expand by sensing the thermal field from the body of a living creature. SMA can absorb energy owing to its pseudoelastic behavior, due to the presence of hysteresis it can absorb impact energy. Figures 1.4–1.7 are some high strain applications of shape memory alloy such as sock absorber, golf stick, tennis racket and sports shoes.



FIGURE 1.4: SMA Shock Absorber



FIGURE 1.5: SMA application in Golf-stick



FIGURE 1.6: Tennis Racket of SMA strip



FIGURE 1.7: Sports shoes of SMA

1.3 Porous Shape Memory Alloy

Lately porous SMA materials has been given much attention due to its addition advantage over the bulk SMA materials. It combines unique properties of SMA (Pseudoelastic and Shape memory effect) with good specific properties, excellent bio-compatibility, good corrosion resistant. Due to these extra-ordinary properties its has wide applications in various fields but currently biomedical fields is a only well explored field. Following figure represents application of porous SMA for varying stiffness implants, where the stiffness can be controlled by changing hole size. An ‘alterable stiffness’ implant might help the bone to heal faster, thus able to bear weight earlier and avoid a follow-on operation. Currently, this alteration is only possible with a biodegradable implant, ‘fixateur externe’ or a second surgery. Therefore, an ‘alterable stiffness’ implant made of NiTi-SMA has been developed to alter the stiffness of the implant with contactless heat induction.

From above explanation it is well understood that shape memory alloy has potential application in various filed such as aerospace, automotive and biomedical industry. Along with that a SMA derivative porous SMA is discussed which as some added advantage over parent SMA , So for utilising these extra-ordinary properties of these material there is a

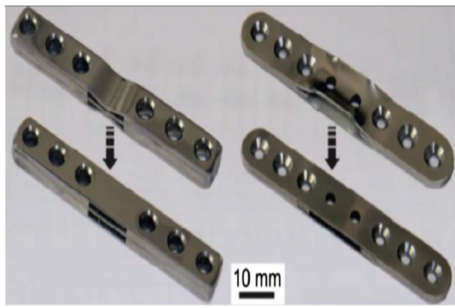


FIGURE 1.8: Alterable stiffness medical implant
Ronny Pfeifera [70]

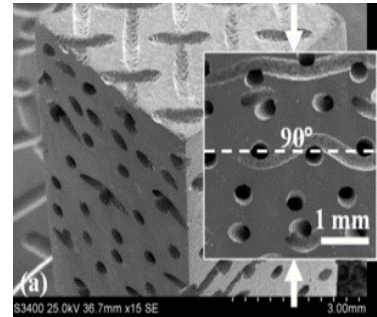


FIGURE 1.9: Porous SMA unit cell

need to explore such material. A regorous literature is presented in next tempeeraure for complete undertanding of shape memory alloy.

Chapter 2

Literature Review

2.1 Literature

Shape memory alloy are the novel materials, which was first discovered by Olander [63]. Shape memory alloy is a special class of material which is capable of undergoing a reversible solid to solid phase transformation under thermal/mechanical loading which may result in large deformation and inelastic stress of 1-8%. The term 'Shape Memory Alloy' was first introduced by Vernon and Vernon [87] but no focus was given until [88, 44] revealed extra-ordinary characteristic of remmembering its original shape. Since the discovery of Shape memory effect and pseudoelastic behaviour the demand for SMAs in different areas of engineering and science field has arises such as: Automotive [23, 83, 21, 44], Aerospace [89, 40, 57], Strcutural applications, Vibration dampers Casciati et al. [22], Energy absorption Zhao et al. [92], Robotics [69, 77, 81, 54] and Biomedical [17, 66, 79, 53]. For detailed application of SMA interesting readers are suggested to follow a review article on SMA applications by Mohd et al. [58].

Although SMA has widespread applications in discrete areas but understanding its behaviour is a challangeing task. So several constitutive model have been developed for predicting complex coupled field paths by considering thermodynamic framework and phase diagram Mathematics et al. [55], D C Lagoudas and Qidwai [30], Boyd and Lagoudas [19], Bri [1]. Boyd and Lagoudas [19]developed first model which accounts martensitic reorientation along with martensitic transformation. D C Lagoudas and Qidwai [30]proposed a polynomial hardening model in his work and comapred results with exponential and cosine hardening model. Later on some models were also developed by implemeting mathmatical model into finite element frame work [68, 67, 64, 26].

Further to investigate the behavior of SMA and optimize its properties both experimental and computational focus has been given under different thermomechanical loading conditions. In this regard vibration control capability of SMA analysed by Damanpack et al. [31] on integrating SMA layers in Isotropic elastic beam subjected to transverse impulse load and influence of location, thickness, test temperature has studied. Gholampour et al. [38]described damping capacity of SMA bars by using into steel structures compared a elastoplastic model with a model having SMA members. A one dimensional constitutive model is proposed by Yu et al. [90]considering both inelastic strain.i.e transformation strain and transformation- induced plastic strain, effect of temperature on residual strain, hysteresis width and martensite start stress is investigated. [46, 45] studied the non-linear dynamic response of SMA sandwich beam by adopting one dimensional constitutive model propoed by Brinson. They compared the damped response of bulk SMA with SMA integrated composite beam based on higher order finite element theory. As far as SMA concern its mechanical properties and microstructure changes with strain rate,Under quasi-static loading condition martensite start stress and work hardening increases with increase in strain rate [85, 75]. Literature depicts that SMA has potentials under transeint loading conditions also, So it is likely to figure out behaviour of SMA in different strain regime. But for exploring mechanical proprieties in dynamic loading conditions control of strain rate is a challanging task. [27, 59] performed a experimental investigation for strain rate dependency of SMA and used a SHPB set-up for controlling strain rate. Tobushi [85] observed the influence of strain rate on superelastic behaviour of SMA for test different temperatures and number of cycles. Also High strain rate and very high strain rate response of porous SMA has been investigated by [59, 60, 5]. Nemat-nasser et al. [60] carried out a experimental study for undetstanding dynamic plastic response of NiTi for defferent strain regimes at a temperature of 296K. A mini-Hopkison pressure bar is used for investigated stress induced martensite formation at strain rates greater than 10000/s. Adharapurapu et al. [5] performed both tension and compression tests for quasi-static and dynamic loading condition for investigating the effect of temperature on stress-strain response.

Lately porous shape memory alloys has attracted the researchers owing to their capability to combine existing propeity of bulk SMA with properties of porous shape memory alloys such as light weight,excellent bio-compatibility [76, 41, 10],higher energy absorption capability Zhao et al. [92] and high corrosion resistance [82, 41]. Due to its good specific properties Porous SMA has potential application such as bone-implant Li et al. [52],energy absorbing device Zhao et al. [92]and vibration dampers . But fabrication of porous SMA is a challenging task,thanks to the researhers [28, 11, 51]for their active contribution on fabricating/processing methods due to such endeavours now a days fabrication is possible

rather easily. Further several methods has been investigated for creating 2D orthogonal microchannels Neurohr and Dunand [62] 3D-interconnected microchannels[14, 15, 16] in NiTi structures.

Having such good properties there was a continuous quest for modelling of porous SMAs. A 3D thermodynamically constitutive model was proposed by [8, 7] for accounting the effect of porosity and plasticity on pseudoelastic and shape memory effect of porous SMA. De Giorgi et al. [33] employed unit cell finite element method and micromechanics averaging based on Mori-Tanaka approach for accouting periodic distribution and random distribution of pores in SMA matrix repectively for predicting overall thermomechanical behaviour. Panico and Brinson [65] developed a micromechanical model based on representative volume element(RVE) and implemented in a finite element frame work for studying the complex interaction of pores,local phase transformation charaterstics and macroscale response. [73, 86]performed a micromechanical study on the influence of porosity, shape, size and oreintation of pores in energy absorption capability mainly.In this work effect of open and closed porosity is also investigated. [39, 13, 12]carried out Extensive study for investigating the fatigue characterstics of porous NiTi. [65, 61] experimentally investigated the stress-strain response of porous SMA under quasi-static and dynamic loading conditions for 12% porosity with different test temperature.

2.2 Technical Challenges

Owing to its extra-ordinary properties SMA has variety of application in various fields of engineering and science. Which attracted researcher a lot in the past few decades. For exploring this material plenty of work has been carried for small strain rate loading condition and some of work focussed on high strain rate behavior of these materials. Lately porous SMA a derivative of SMA has fascinated people due to its good specific properties, light weight and good-bio compatibilty. Several work has been carried out for utilising these excellent properties but majority of work is limited to quasi-static loading condition. Mechanical behavior of these material under high strain rate loading conditions is still unclear so far, So there is an impetus towards understanding effect of heterogeneity on high strain rate behavior of porous SMA under dynamic loading.

2.3 Research objectives

The objective of the present study is to understand the role of geometric and loading parameter in porous SMA under dynamic loading conditions. Therefore, our aim is to develop a numerical framework that will simulate the dynamic behavior of porous SMA. We will address the effect of geometry and loading parameter particularly shape, size and distribution of pore along with different strain rate. To achieve this we have some tasks which are described below:

Task carried for achieving research objectives:

- Understanding the thermomechanical behavior of shape memory alloy.
- Development of explicit finite element framework based model.
- Generation of different porous SMA structures .
- Simulation of mechanical behavior of porous SMA for different geometric and loading parameter.
- Investigation of the effect of heterogeneity and loading rate on energy absorption characteristics.

2.4 Scope of present study and progress report organization

The goal of present work is to develop a robust finite element model for investigating the role of heterogeneity of mechanical behavior of porous shape memory alloy composites. Therefore, in Chapter 3 we presented a numerical framework to understand dynamic response of porous SMA. An explicit dynamic finite element framework has been developed for simulating dynamic response of material. In Chapter 4 mechanical, thermal properties are discussed and presented initial and boundary conditions in this chapter. Along with result of the study has been explored such as effect of strain rate, porosity of material behavior and energy characteristics of material. At last in Chapter 5, we concluded research finding of present work and future work plan.

Chapter 3

Formulation of Computational Framework

In this section we develop mathematical model to understand energy absorption behavior of shape memory alloy material in presence of pores. We particularly employ explicit dynamic finite element scheme to simulate the transient response. We briefly describe the finite element formulation. Later we show the detail implementation of the SMA constitutive equation and numerical procedure to extract the SMA response.

3.1 Governing equations

In the given a body B is shown whose boundary is represented by ∂B_u . Suppose any point on the boundary x whose displacement is given by u and traction applied on the same point is given by t , mathematically this can be rewritten as follows:

$$\begin{aligned} u(x, t); \quad x \in \partial B_u \\ t(x, t); \quad x \in \partial B_t \end{aligned}$$

- **Strain-Displacement equation** A relationship which connects displacement field with strain is called as strain displacement relationship. Mathematically which can be represented as follows:

$$\boldsymbol{\epsilon} = \frac{1}{2}(\boldsymbol{\nabla}u + \boldsymbol{\nabla}u^T) \quad (3.1)$$

Where u is the displacement vector and ϵ represents strain tensor

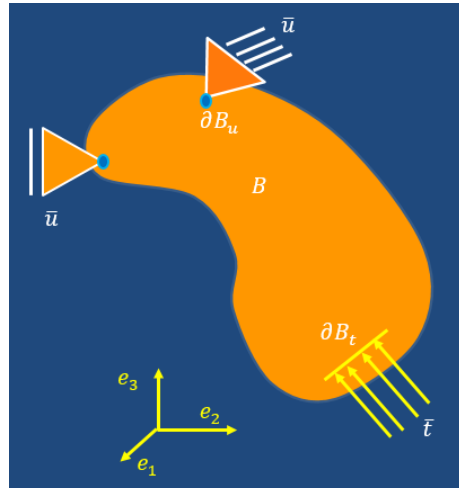


FIGURE 3.1: Schematic of generic problem in solid mechanics

- **Balance of linear momentum** The law of conservation of linear momentum states that the rate of change of linear momentum of a continuum body is equal to the total sum of surface and body forces applied to it.

$$\nabla \cdot \sigma = \rho \ddot{u} \quad (3.2)$$

- **Constitutive relation** Constitutive equations are mathematical models intended to describe the principal features of a material behavior in an idealized form.

$$\sigma = \rho \frac{\partial \psi}{\partial \epsilon} \quad (3.3)$$

Where ψ represents Helmholtz free energy function.

- **Boundary conditions**

-**Traction** or natural boundary conditions: For tractions \bar{t} imposed on the portion of the surface of the body ∂B_t :

$$n_i \sigma_{ij} = t_j = \bar{t}_j \quad (3.4)$$

-**Displacement** or essential boundary conditions: For displacements \bar{u} imposed on the portion of the surface of the body ∂B_u , this includes the supports for which we have $\bar{u} = 0$:

$$u_i = \bar{u}_i \quad (3.5)$$

3.2 Explicit finite element formulation

3.2.1 Variational formulation

In this section, variational formulation for a porous SMA quad element is developed. By adopting principle of virtual work condition for equilibrium condition at the element level can be derived and which can be stated as:

$$\delta W_{kin} - \delta W_{int} + \delta W_{ext} = 0, \quad (3.6)$$

where δW_{kin} , δW_{int} and δW_{ext} is the variation of kinetic energy, internal energy and external work done, can be written as follows:

$$\delta W_{kin} = \int_{V_e} \rho_e (\delta u^T \ddot{u}) dV_e \quad (3.7)$$

$$\delta W_{int} = \int_{V_e} \delta \epsilon^T \sigma_e dV_e \quad (3.8)$$

$$\delta W_{ext} = \int_l \delta u^T F_{ext} dx \quad (3.9)$$

3.2.2 Finite element model

The weak form of equation of motion for quad element is presented in previous section which is used here for finite element formulation. The domain is discretized in n number of quad element and the displacement is interpolated as follow:

$$u = \sum_{i=1}^4 u_i \psi_i \quad (3.10)$$

Where ψ_i is the linear Lagrange interpolation function. Using proposed displacement field function these quantities can be expressed as nodal variable:

$$\{u\} = [N] \{\bar{u}\} \quad (3.11)$$

where $\{u\}$ is displacement vector, $\{\bar{u}\}$ is nodal displacement vector and $[N]$ represents shape function.

$$\{\epsilon\} = \frac{\partial}{\partial x} \{[N] \{\bar{u}\}\}, \quad \{\epsilon\} = [B] \{\bar{u}\} \quad (3.12)$$

$$\{\delta \epsilon\} = [B] \{\delta \bar{u}\} \quad (3.13)$$

$$\delta W_{kin} = \delta \bar{u}^T \int_{V_e} \rho_e [N]^T [N] dV_e \quad (3.14)$$

$$\delta W_{int} = \delta \bar{u}^T \int_{V_e} [B]^T [\sigma] dV_e, \quad \delta W_{int} = \delta \bar{u}^T F_{int} \quad (3.15)$$

$$\delta W_{ext} = \delta \bar{u}^T \int_{V_e} [N]^T F_{ext} dV_e \quad (3.16)$$

On putting all these values in equation (1) we get,

$$[M]_E \{\ddot{u}\} = F_{ext} - F_{int} \quad (3.17)$$

where

$$[M]_E = \int_{V_e} \rho_e [N]^T [N] dV_e, \quad F_{int} = \int_{V_e} [B]^T [\sigma] dV_e \quad (3.18)$$

equation(11) is the non-linear governing equation of SMA Plate element which can be utilised to develop global finite element vectors and matrices by assembly and imposition of boundary which results in:

$$\mathbf{M} \ddot{\mathbf{u}} = \mathbf{F}_{ext} - \mathbf{F}_{int} \quad (3.19)$$

\mathbf{M} denotes mass matrix, \mathbf{F}_{ext} and \mathbf{F}_{int} denotes external load vector and internal load vector respectively.

3.2.3 Explicit Time Integration scheme

Equation(3.13) is integrated explicitly using central difference time integration scheme to calculate global velocity $\dot{\mathbf{u}}$ and displacement vector \mathbf{u}

$$\dot{u}^{n+1} = \dot{u}^n + \frac{1}{2} \Delta t [\ddot{u}^n + \ddot{u}^{n+1}] \quad (3.20)$$

$$u^{n+1} = u^n + \frac{1}{2} \Delta t \dot{u}^n + \frac{1}{2} \Delta t^2 \ddot{u} \quad (3.21)$$

where $(:)^{n+1}$ represents values at time step $t = t^{n+1}$ while $(:)^n$ denotes value at time step $t = t^{n+1}$

Input :Applied Velocity $\dot{u}(x, t)$
Output :Nodal displacement $u(x, t)$
1. Initial condition:set $\dot{u}(x, t = 0)$
2. Calculate Mass matrix \mathbf{M}
3. Evaluate time step Δt from CFL condition;
4. Set loop variables: n_{max} or t_{max} ;
while $t < t_{max}$ or $n < n_{max}$ do
5 Internal force Calculation \mathbf{F}_{int}
6.External Force evaluation \mathbf{F}_{ext}
7.Calculate Acceleration $\ddot{u}^{n+1} = \mathbf{M}^{-1} [\mathbf{F}_{int} - \mathbf{F}_{ext}]$
8. Update Nodal Velocity $\dot{\mathbf{u}}^{n+1}$
9. Essential Boundary conditions $\dot{\mathbf{u}}^{n+1}(x = \bar{x}, t)$
10.Update Nodal Displacement \mathbf{u}^{n+1}
11. Update loop variables

Explicit integration scheme are conditionally stable scheme such that time step size must be less than a critical time step size. Critical time step is defined as time for wave to travel from one end to another end of the element. By following the Courant-Friedrichs-Lowy(CFL) condition the time step size for explicit marching can be calculated as:

$$\Delta t = \psi \frac{\Delta x}{c_d}$$

where ψ is the Courant number, Δx is the minimum element length and c_d is wave speed in the element. For the simulations presented in this paper, we have chosen $\psi = 0.05$ so that the solutions remain well within the stable regime

3.3 SMA Constitutive Model

In the present work, for studying mechanical behaviour of porous SMA in the small-strain regime a SMA constitutive model developed by D C Lagoudas and Qidwai [30] based on thermodynamic framework of [19]is employed. Total Gibbs free energy 'G'of SMA is give by:

$$\mathbf{G}(\sigma, \zeta, T, \epsilon^t) = -\frac{1}{2} \frac{1}{\rho} \sigma : S : \sigma - \frac{1}{\rho} \sigma : [\alpha(T - T_0) + \epsilon^t] + c[(T - T_0) - T \ln \frac{T}{T_0} - s_0 T + u_0 + f(\zeta)] \quad (3.22)$$

Where material parameter S , α , c , u_0 and s_0 are Compliance tensor, effective thermal expansion tensor, specific heat, internal energy and entropy respectively at ambeint conditions. σ , ζ , ϵ^t , T , T_0 and $f(\zeta)$ are Cauchy stress tensor, martensitic volume fraction, transformation strain tensor, current teperature, reference temperature and harding function. All the effective propeities can be represented in terms of pure phase and martensitic volume fraction ' ζ :

$$S(\zeta) = S^A + \zeta(S^M - S^A)$$

$$\alpha(\zeta) = \alpha^A + \zeta(\alpha^M - \alpha^A)$$

$$s_0(\zeta) = s_0^A + \zeta(s_0^M - s_0^A)$$

$u_0(\zeta) = u_0^A + \zeta(u_0^M - u_0^A)$ Relation between Gibbs free energy and internal energy is given by Legendre transformation as:

$$\mathbf{G}(\sigma, \zeta, s, \epsilon^t) = G + Ts + \frac{1}{\rho}\sigma : \epsilon \quad (3.23)$$

By putting the value of G and u into the first and seond law of thermodynamics and by following Coleman and Noll procedue total strain tensor and entropy can be represented as:

$$\epsilon = S : \sigma + \alpha(T - T_0) + \epsilon^t \quad (3.24)$$

$$s = \frac{1}{\rho}\sigma : \alpha + c \ln\left(\frac{T}{T_0}\right) \quad (3.25)$$

3.3.1 Evolution of Internal Variables

After defining the expression for total strain and entropy now need to define evolution equation of internal variables (ϵ^t, ζ),in this adopted model it is assumed that phase transformation occurs only due to change in martensite volume fraction not by oreintation of martensitic variant.Considering this assumption relationship can be developed between transformation strain and martensitic volume fraction called as flow rule:

$$\dot{\epsilon}^t = \Lambda \dot{\zeta} \quad (3.26)$$

where Λ is a second order transformtion tensor represents direction of transformation strain which can be calculated forward/reversed transformation as follows:

$$\begin{cases} \Lambda = \frac{3}{2}H\frac{\sigma'}{\sigma_{eff}}, & \dot{\zeta} > 0. \\ H\frac{\epsilon_{t-r}}{\epsilon_{eff}}, & \dot{\zeta} < 0. \end{cases} \quad (3.27)$$

H denotes the maximum transformation strain, ϵ_{t_r} is the transformation stain tensor.

$$\sigma_{eff} = \sqrt{\frac{3}{2}||\sigma'||} \quad \sigma' = \sigma - \frac{1}{3}(tr\sigma) \quad \sigma_{eff} = \sqrt{\frac{3}{2}||\sigma'||} \quad (3.28)$$

endequation Using equation by (5) total energy dissipation rate can be written as:

$$(\sigma : \Lambda - \rho \partial_\zeta G)\dot{\zeta} = \pi \dot{\zeta} \geq 0 \quad (3.29)$$

Where π is the thermodynamic driving force for martensitic volume fraction ' ζ ',which is give by:

$$\pi = \sigma : \Lambda + \frac{1}{2}\sigma : \Delta S : \sigma + \sigma : \Delta\alpha(T - T_0) - \rho\Delta c[(T - T_0) - T\ln(\frac{1}{2})] + \rho\Delta S_0 T - \frac{\partial f}{\partial \zeta} \quad (3.30)$$

Now let's introduce a transformation function ' ϕ 'use decides wether Phase transformation will occure or not during loading/unloading situations:

$$\phi = \begin{cases} \pi - Y, & \text{if } \dot{\zeta} > 0 \\ -\pi - Y, & \text{if } \dot{\zeta} < 0 \end{cases} \quad (3.31)$$

Inequility constraint on the evolution of martensitic volume fraction can be expressed by so called Kurash Kuhn-Tucker conditions,which are given below for both forward/reverse loading condition:

$$\dot{\zeta} \geq 0; \quad \phi(\sigma, \zeta, T) = \pi - Y \leq 0; \quad \phi \dot{\zeta} = 0; \quad (3.32)$$

$$\dot{\zeta} \leq 0; \quad \phi(\sigma, \zeta, T) = \pi - Y \leq 0; \quad \phi \dot{\zeta} = 0; \quad (3.33)$$

A quadratic hardening function is assumed in this model which is responsible for transformation induced hardening in Shape Memory alloy materials:

$$f(\zeta) = \begin{cases} \frac{1}{2}\rho b^M \zeta^2 + (\mu_1 + \mu_2)\zeta, & \dot{\zeta} > 0 \\ \frac{1}{2}\rho b^A \zeta^2 + (\mu_1 - \mu_2)\zeta, & \dot{\zeta} < 0 \end{cases} \quad (3.34)$$

Where $\rho b^M, \rho b^A, \mu_1$ and μ_2 are the strain hardening constant.

Input :Strain $\epsilon(x, t)$

Output: Stress $\sigma(x, t)$

1. Initial conditions, Let $k = 0, \zeta_{n+1}^{(0)} = \zeta_n, \epsilon_{n+1}^{t(0)} = \epsilon_n^t, S_{n+1}^{(0)} = S_n, \alpha_{n+1}^{(0)} = \alpha_n$
2. Calculate thermoelastic prediction and evaluate transformation function

$$\begin{aligned} \sigma_{n+1}^{(k)} &= S_{n+1}^{(k)-1} : [\epsilon_{n+1} - \alpha_{n+1}^k (T_{n+1} - T_0) - \epsilon_{n+1}^{t(k)}] \\ \phi_{n+1}^{(k)} &= \phi[\sigma_{n+1}^{(k)}, T_{n+1}, \zeta_{n+1}^{(k)}] \end{aligned}$$

If $|\phi_{n+1}^{(k)}| \geq \text{Tolerance}$ then

Enter Into Inelastic Zone

Else

Enter Into Elastic Zone

1. Calculate change in martensitic volume fraction and transformation strain

$$\Delta\zeta_{n+1}^{(k)} = \frac{\phi_{n+1}^{(k)}}{\frac{\partial\phi_{n+1}^{(k)}}{\partial\sigma} : S_{n+1}^{(k)-1} : \frac{\partial\phi_{n+1}^{(k)}}{\partial\sigma} - \frac{\partial\phi_{n+1}^{(k)}}{\partial\zeta}}$$

$$\Delta\epsilon_{n+1}^{t(k)} = \Delta\zeta_{n+1}^{(k)} \Lambda_{n+1}^{(k)}$$

1. Update martensite volume fraction and transformation strain

$$\zeta_{n+1}^{(k+1)} = \zeta_{n+1}^{(k)} + \Delta\zeta_{n+1}^{(k)}$$

$$\epsilon_{n+1}^{t(k+1)} = \epsilon_{n+1}^{t(k)} + \Delta\epsilon_{n+1}^{t(k)}$$

Chapter 4

High Strain Behavior of Porous Shape Memory Alloy

4.1 Introduction

The explicit dynamic non-linear finite element framework as elucidated in last chapter has been adopted for simulating high strain rate behaviour of bulk and porous SMA. The rate sensitivity of any constituent material is excluded from our model. Along with that we have considered only small deformation mechanism. A parametric study has been performed for investigating the effect of loading profile and shape, size and distribution of porosity. Both the end of the specimen are subjected to same velocity but in opposite direction, The developed numerical framework can produce snapshots of different quantities of interest, such as different strain rate, Thus it enables the investigation of relation between global response and local response.

This chapter is organised in following manner; In section 4.1 computational domain with boundary condition is described, in section 4.2 effect of strain rate for a given porosity is investigated and in section 4.3 effect of porosity on material behavior for given strain rate is investigated.

4.2 Problem definition

In the current study axial impact/high strain rate behaviour of porous SMA is investigated by considering two dimensional computation domain which represents the specimen. Figure 4.1 shows a porous specimen of length L and width W having a aspect ratio $\phi = \frac{L}{W}$. In the present study Aspt ratio $\phi = 3$, $H = 12\text{cm}$ and $W = 3\text{cm}$ is same throughout, if there will be any change we will mention it accordingly. To create homogeneous strain rate loading conditon domain is subjected to velocity boundary condition from both ends. Initial loading conditions:

$$\left\{ \begin{array}{l} \dot{u}(x, y, 0) = 0 \\ \dot{v}(x, y, 0) = -\dot{\epsilon}y \end{array} \right\} \text{ for } \left\{ \begin{array}{l} x \in [-\frac{W}{2}, \frac{W}{2}] \\ y \in [-\frac{H}{2}, \frac{H}{2}] \end{array} \right\}$$

Boundary conditions:

$$\dot{u}(x, \pm \frac{H}{2}, 0) = \mp V$$

If V is the initial applied velocity then Strain rate can be define as:

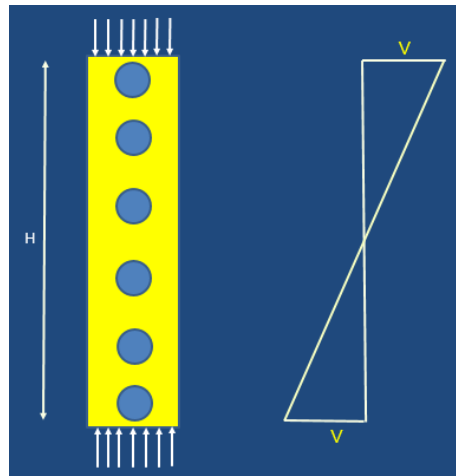


FIGURE 4.1: Homogeneous strain loading condition

$$\dot{\epsilon}(t) = \frac{-2V}{H} \quad (4.1)$$

Now,Normal strain can be calculated as

$$\epsilon(t) = \int_0^t \dot{\epsilon}(t) dt \quad (4.2)$$

Normal stress can be calculated by taking volume average of all stress for entire domain as described in chapter 3, Which accounts microstructural features with in it.

Material Properties	Austanite	Martensite
Young modulus(GPa)	55	46
Poisson ratio	0.33	0.33
$M_s(K)$	-	245
$M_f(K)$	-	230
$A_s(K)$	270	-
$A_f(K)$	280	-

Hardening parameter H=0.056

4.3 Results and discussions

The main of this article is to get the constitutive behavior of porous SMA composites at macroscale with different loading pattern and variations in microstructure and material parameters. Main results are discussed below:

In the first observation it was observed that constitutive behaviour of porous SMA is different for quasi-static and dynamic loading regimes which can be observe from figure 4.2. It quite clear from the figure that for dynamic strain rate regime the stiffness of the same material is high in comparison to its quasi-static behaviour. This is due to the fact that under dynamic loading regimes occurrence of dynamic stiffness due to inertia effect augments the material stiffness.

4.3.1 Variation of material response for different strain rates at fixed porosity

In initial study a specimen with no porosity having length H=12cm and width W=3cm is subjected to a velocity V from both of the edges. Results observed can be seen from Figure 4.3, which shows stres-strain response of material for a range($10^2 - 10^5$)of strain rate. It is investigated from figure that stiffness is almost same for all strain rates because of the absence of inertial effects. Another observation is that on increasing stran rate toughness of the material is decreasing. This is because at higher strain a low stiff phase martensite is completely forming with in the material which results in reduced stress value

in later part of the curve. In the next step porosity is introduced with in the specimen keeping its dimensions unchanged. For creating a specimen with 13.02% porosity six holes having diameter $d=1.0\text{cm}$ are intriduced in the regular speimen. Specimen subjected to velocity boundary condition at its both of the ends. Simulation is performed in parallel compuational environment which are shown in Fig.4.4 , it is observed that the stiffness of the material is increasing for higher strain rates, This is because of the presence of dynamic stiffness augments in total material stiffness. Along with that for lower strain rate regimes material toughness in lowering but after 10^4 strain the toughness is not changing.

Further for observing the effect of porosity a porous specimen having similiar dimensions as above and having six holes with 1.5cm diameter is used. By implementing it into parallel compuation environment,stress-strain curved has been plotted for different value of strain rate. Figure 4.5 is represantaion of material behavior for 29.43% porosity. The trend followed by the material is almost as that in previous case but at higher strain rates material is reaching towards bulk material behaviour. So, conlusion of these cases is that irrespective of porosity material is reaching towards its parent material behavior.

Further effect of strain rate on energy absorption characterstics is explored by extracting data from above results and calculating the area under strain curve which is show in figure 4.6. For bulk material energy dissipation is decreasing continuously. But in case of 13.02% porosity behavior is quite dramatic, for quasi-static regime ebergy absorption is well below

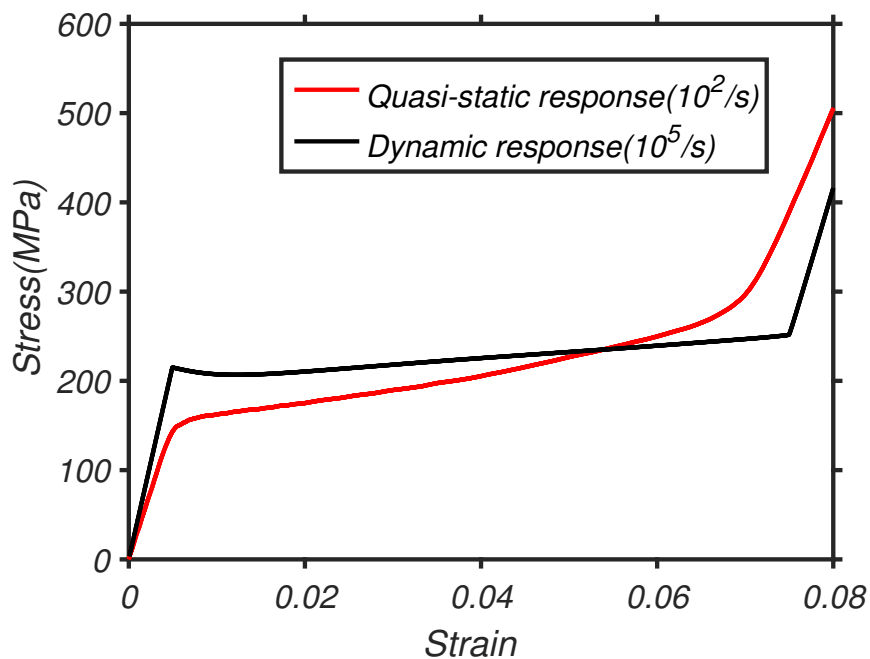


FIGURE 4.2: Quasi-static and Dynamic behavior of porous SMA

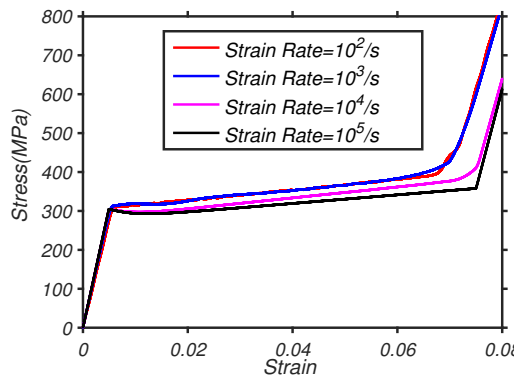


FIGURE 4.3: stress-strain behavior of bulk SMA

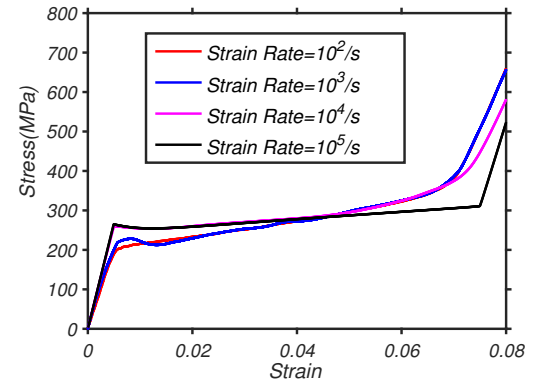


FIGURE 4.4: stress-strain behavior of 13.08% porosity level

but in dynamic regimes it is going above for some value of strain then after that coming at the same level.

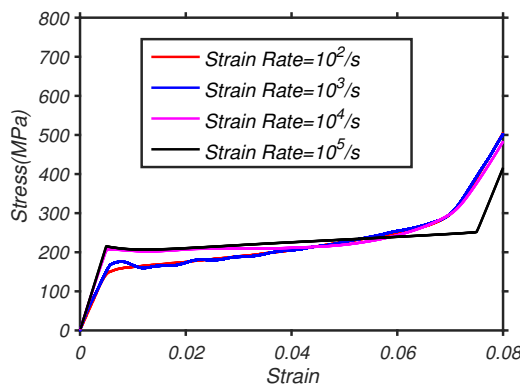


FIGURE 4.5: stress-strain behavior of 29.43% porosity level

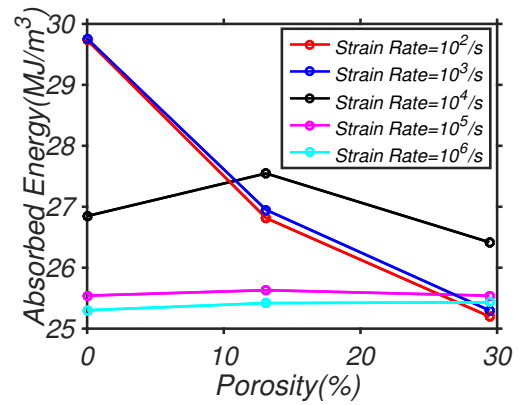


FIGURE 4.6: Energy absorption characteristics of Porous SMA for different strain rate

4.3.2 Stress-strain response of material with varying porosity at fixed strain rate

In previous section we have seen the reponse of material for different porosity but in this section we will observe the response of material for varying porosity at a given value of strain rate. In this section keeping all the parameter same different graphs has been plotted for stress vs strain at different porosity at fixed strain. Figure 4.7 is the response of material at a strain rate $10^3/s$, it is quite clear that for a given strain when stiffness

and toughness of the material is decreasing with increasing porosity level. In figure 4.8 constitutive behavior is observed at a strain rate of $10^4/s$, the behaviour is almost same as that of previous case stress strain curve are coming closure. But when strain is increased above $10^4/s$ the behaviour is just opposite bulk material is lossing its strength .i.e is due to complete formation of martensite, because martensite is phase of lower strength. At last for a strain rate of $10^5/s$ all structure are behavior like bulk SMA,all has same strength as well as same toughness,which is quite strange behavior.

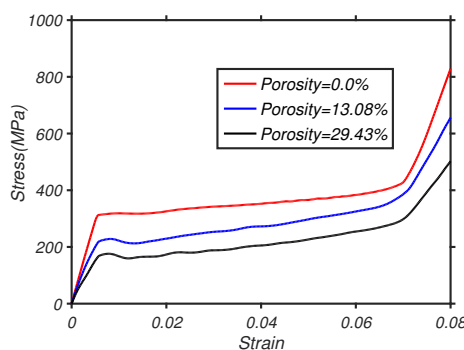


FIGURE 4.7: Stress strain rate behavior at 10^3 strain rate

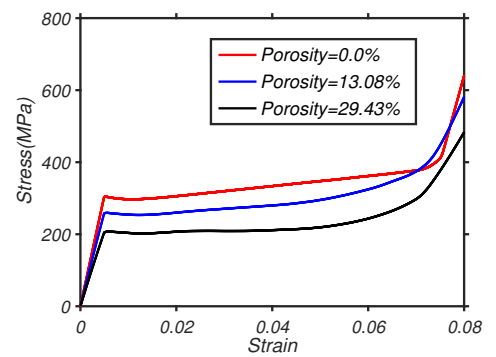


FIGURE 4.8: Stress strain rate behavior at 10^4 strain rate

As far as energy concern absorbed energy is plotted against strain rate for different porosity level in quasi-static regimes energy absorbed by regular material is more in comparison to porous material but in dynamic regime energy absorbed by all material is same this because of complete and almost uniform formation of martensitic phase, it means no matter which structure you are adopting it will absorbed same amount of energy.

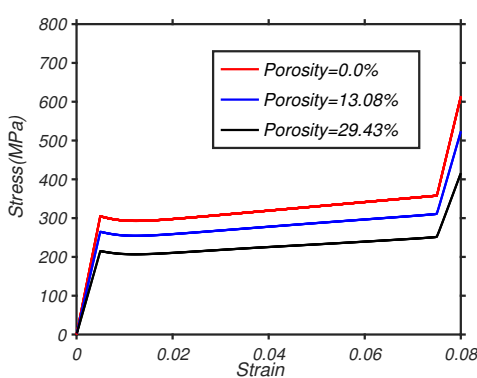


FIGURE 4.9: Stress strain rate behavior at 10^5 strain rate

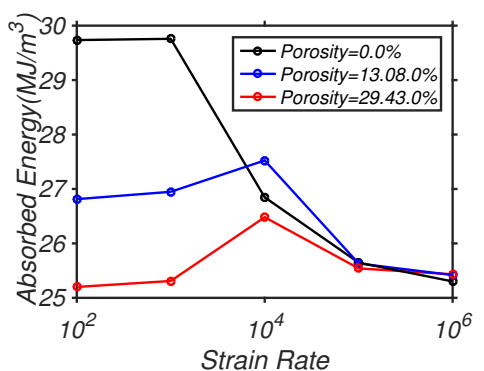


FIGURE 4.10: Energy absorption characteristics of Porous SMA for different porosity level

4.3.3 Effect of strain rate on strength ratio of porous SMA

In this section effect of strain rate on strength ratio has been observed. Two specimen having pore diameter 1.5 cm and 1.0 cm by keeping other dimensions same as above are subjected to different of strain rate ($10^2/s - 10^6/s$). The porosity for the specimen is

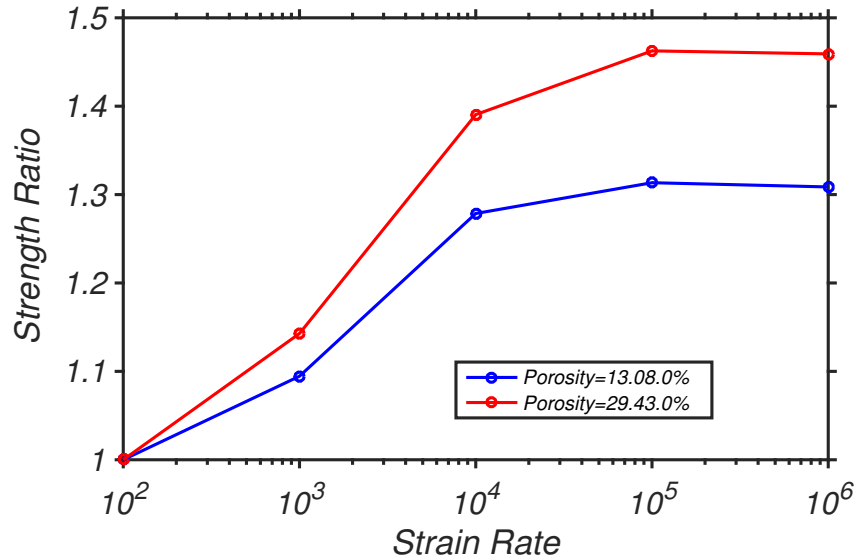


FIGURE 4.11: Variation of strength ratio with strain rate

13.08% and 29.43% respectively, It is observed that with increasing strain rate strength ratio is increasing. The effect is more predominant in case of higher porosity this is because of the presence of inertia forces.

Chapter 5

Conclusion and Future Plan

5.1 Findings of present work

In the present study we are particularly focused on two aspects i.e. effect of heterogeneity and loading parameters on material behavior. Therefore, for studying the effect of heterogeneity(pores) and strain rate behavior of material we developed a robust numerical framework. Several porous SMA strcuture has been developed for different porosity and implemented into the finite element framework. Following are some preliminary findings of the present work:

- As a basic study comparison between quasi-static and dynamic response of the porous SMA is observed. Which shows that the dynamic response of material deviates from quasi-static response.
- Investigated the effect of strain rate on material stiffness. It was observed that stiffness of the porous SMA structure is increasing with increase in strain rate.
- Investigated the effect of porosity and strain rate on phase transformation characteristics which explains evolution of martensite zone with in the material.
- In further study its is observed that absorbed energy is decreasing with strain rate and porosity initially but at higher value of strain rate amount of absorbed energy is same irrespective of porosity level.
- Variation of transformation stress ratio with strain is plotted which shows that stress ratio is increasing initially with strain rate but at higher strain rate saturation is achieved and stress ratio remains almost same.

5.2 Future work Plan

So far we have studied the effect uniformly distributed circular pores over the material domain. Along with the effect of porosity we have also studied the effect of strain rate on mechanical behavior of material. As a further work our plane is :

- To understand the effect of various shape, size and distribution of porosity on mechanical behavior of porous SMA.
- Along with that as a applied work focus will be given to impact and ballast application of these materials which will have potential application in various safety devices such as car crash structure, bumpers, design of armor and landing gear application.

Bibliography

- One-Dimensional Constructive Behavior of Shape Memory Alloys:Thermomechanical Derivation with Non-Constant Material Functions and Redefined Martensite Internal Variable. 1992.
- Modeling of the thermomechanical behavior of porous shape memory alloys. 38(48-49): 8653–8671, 2001. ISSN 00207683.
- Computational modeling of porous shape memory alloys. 45(21):5613–5626, 2008. ISSN 00207683.
- ABAQUS. *Abaqus 6.11 Online Documentation*. Dassault Systemes, 2011.
- R. R. Adharapurapu, F. Jiang, K. S. Vecchio, and G. T. Gray. Response of NiTi shape memory alloy at high strain rate: A systematic investigation of temperature effects on tension-compression asymmetry. 54(17):4609–4620, 2006. ISSN 13596454.
- D. R. Armentrout. *An analysis of the behavior of steel liner anchorages*. PhD thesis, University of Tennessee, 1981.
- M. Ashrafi, J. Arghavani, R. Naghdabadi, and F. Auricchio. A three-dimensional phenomenological constitutive model for porous shape memory alloys including plasticity effects. 27(5):608–624, 2016. ISSN 1045-389X.
- M. J. Ashrafi, J. Arghavani, R. Naghdabadi, and S. Sohrabpour. A 3-D constitutive model for pressure-dependent phase transformation of porous shape memory alloys. 42: 292–310, 2015. ISSN 18780180.
- J. R. Ashwin Rao, A.R. Srinivasa. *Design of Shape Memory Alloy (SMA) Actuators*. Springer, 2015.
- R. A. Ayers, S. J. Simske, T. A. Bateman, A. Petkus, R. L. C. Sachdeva, and V. E. Gyunter. Effect of nitinol implant porosity on cranial bone ingrowth and apposition after 6 weeks. 45(1):42–47, 1999. ISSN 00219304.

- A. Bansiddhi. Shape-memory NiTi – Nb foams. 2009.
- S. Bernard, V. K. Balla, S. Bose, and A. Bandyopadhyay. Rotating bending fatigue response of laser processed porous NiTi alloy. 31(4):815–820, 2011. ISSN 09284931.
- S. Bernard, V. Krishna Balla, S. Bose, and A. Bandyopadhyay. Compression fatigue behavior of laser processed porous NiTi alloy. 13:62–68, 2012. ISSN 17516161.
- C. Bewerse, L. C. Brinson, and D. C. Dunand. Journal of Materials Processing Technology NiTi with 3D-interconnected microchannels produced by liquid phase sintering and electrochemical dissolution of steel tubes. 214:1895–1899, 2014.
- C. Bewerse, A. A. Emery, L. C. Brinson, and D. C. Dunand. A NiTi porous structure with 3D interconnected microchannels using steel wire spaceholders. 634:153–160, 2015. ISSN 0921-5093.
- C. Bewerse, L. C. Brinson, and D. C. Dunand. Porous shape-memory NiTi-Nb with microchannel arrays. 115:83–93, 2016. ISSN 1359-6454.
- N. B.Morgan. Medical shape memory alloy applications - The market and its products. 378(1-2 SPEC. ISS.):16–23, 2004. ISSN 09215093.
- A. Bower. *Applied Mechanics of Solids*. Taylor and Francis, 2011.
- J. G. Boyd and D. C. Lagoudas. A THERMODYNAMICAL CONSTITUTIVE MODEL FOR SHAPE MEMORY MATERIALS . PART I . THE MONOLITHIC SHAPE MEMORY ALLOY . pages 1–40, 1996.
- R. H. Brown and A. R. Whitlock. Strength of anchor bolts in grouted concrete masonry. *Journal of Structural Engineering*, 109(6):1362–1374, 1983.
- F. Butera. Shape memory actuators. (March):37–40, 2008.
- F. Casciati, L. Faravelli, and C. Fuggini. Acta Mechanica Cable vibration mitigation by added SMA wires. 155:141–155, 2008.
- K. M. Cees Bil and E. J. Abdullah. Wing morphing control with shape memory alloy actuators. 24(7), 2013. ISSN 1045389X.
- Z. Celep. Rectangular plates resting on tensionless elastic foundation. *Journal of Engineering mechanics*, 114(12):2083–2092, 1988.

- S. Chakraborty. An experimental study on the behaviour of steel plate-anchor assembly embedded in concrete under biaxial loading. M.tech thesis, Indian Institute of Technology Kanpur, August 2006.
- Y. Chemisky, A. Duval, E. Patoor, and T. B. Zineb. Mechanics of Materials Constitutive model for shape memory alloys including phase transformation , martensitic reorientation and twins accommodation. 43:361–376, 2011.
- W. W. Chen, Q. Wu, J. H. Kang, and N. A. Winfree. Compressive superelastic behavior of a NiTi shape memory alloy at strain rates of 0 . 001 750 s . 38:8989–8998, 2001.
- C. L. Chu, C. Y. Chung, P. H. Lin, and S. D. Wang. Fabrication of porous NiTi shape memory alloy for hard tissue implants by combustion synthesis. 366:114–119, 2004.
- R. A. Cook and R. E. Klingner. Ductile multiple-anchor steel-to-concrete connections. *Journal of structural engineering*, 118(6):1645–1665, 1992.
- Z. B. D C Lagoudas and M. A. Qidwai. A Unified Thermodynamic Constitutive Model for SMA and Finite Element Analysis of Active Metal Matrix Composites. 3(2):153–179, 1996. ISSN 1075-9417.
- A. R. Damanpack, M. Bodaghi, M. M. Aghdam, and M. Shakeri. On the vibration control capability of shape memory alloy composite beams. 110:325–334, 2014.
- V. N. Damarla. An experimental investigation of performance of steel plate-concrete interfaces under combined action of shear and normal forces. Master's thesis, Indian Institute of Technology Kanpur, July 1999.
- V. G. DeGiorgi, M. a. Qidwai, P. B. Entchev, and D. C. Lagoudas. Modeling of the thermomechanical behavior of porous shape memory alloys. 38(48-49):8653–8671, 2001. ISSN 00207683.
- I. Doghri. Fully implicit integration and consistent tangent modulus in elasto-plasticity. *International Journal for Numerical Methods in Engineering*, 36(22):3915–3932, 1993.
- P. B. Entchev and D. C. Lagoudas. Modeling porous shape memory alloys using micromechanical averaging techniques. 34(1):1–24, 2002. ISSN 01676636.
- FEMA. Interim testing protocols for determining the seismic performance characteristics of structural and nonstructural components. Report 461, Federal Emergency Management Agency, June, 2007.

- J. Furche and R. Elingehausen. Lateral blow-out failure of headed studs near a free edge. *Anchors in Concrete-Design and Behavior*, SP-130, 1991.
- A. A. Gholampour, M. Ghassemieh, and J. Kiani. International Journal of Engineering Science State of the art in nonlinear dynamic analysis of smart structures with SMA members. 75:108–117, 2014.
- A. F. D. G.Ipek Naka and S. Bor. Fatigue behavior of TiNi foams processed by the magnesium space holder technique. 4(20 I I):2017–2023, 2011.
- D. J. Hartl and D. C. Lagoudas. Aerospace applications of shape memory alloys. 221(4): 535–552, 2007. ISSN 1687-9465. doi: 10.1155/2011/501483.
- X. Huang, D. W. Norwich, and M. Ehrlinspiel. Corrosion behavior of Ti-55Ni-1.2Co high stiffness shape memory alloys. 23(7):2630–2634, 2014. ISSN 15441024.
- G. B. J. H. Mabe, F. Calkins. Boeing’s variable geometry chevron,morphing aerostructure for jet noise reduction. pages 1–19, 2006.
- J. J. Kallolil, S. K. Chakrabarti, and R. C. Mishra. Experimental investigation of embedded steel plates in reinforced concrete structures. *Engineering structures*, 20(1):105–112, 1998.
- G. B. Kauffman and I. Mayo. The Story of Nitinol: The Serendipitous Discovery of the Memory Metal and Its Applications. *The Chemical Educator*, 2(2):1–21, 1997. ISSN 1430-4171.
- S. M. R. Khalili, M. Botshekanan Dehkordi, and M. Shariyat. Modeling and transient dynamic analysis of pseudoelastic SMA hybrid composite beam. 219(18):9762–9782, 2013a. ISSN 00963003.
- S. M. R. Khalili, M. B. Dehkordi, E. Carrera, and M. Shariyat. Non-linear dynamic analysis of a sandwich beam with pseudoelastic SMA hybrid composite faces based on higher order finite element theory. *Composite Structures*, 96:243–255, 2013b. ISSN 0263-8223.
- H. Krawinkler, M. Zohrei, B. Lashkari-Irvani, N. Cofie, and H. Hadidi-Tamjed. Recommendations for experimental studies on the seismic behavior of steel components and materials. Report, Department of Civil and Environmental Engineering, Stanford University, September 1983.
- D. Lagoudas. Modeling of thermomechanical response of porous shape memory alloys. 3992:496–508, 2000. ISSN 0277-786X.

- J. Lemaitre and J. L. Chaboche. *Mechanics of Solid Materials*. Cambridge University Press, 1994. ISBN 9780521477581.
- B. Lester, T. Baxevanis, Y. Chemisky, D. Lagoudas, B. Lester, T. Baxevanis, Y. Chemisky, and D. L. Review. Review and Perspectives : Shape Memory Alloy Composite Systems To cite this version : Science Arts & Métiers (SAM). 2015.
- B.-y. Li, L.-j. Rong, and Y.-y. Li. Stress-strain behavior of porous Ni-Ti shape memory intermetallics synthesized from powder sintering. 8:1–4, 2000.
- J. Li, H. Yang, H. Wang, and J. Ruan. Low elastic modulus titanium-nickel scaffolds for bone implants. 34(1):110–114, 2014. ISSN 09284931.
- L. G. Machado and M. A. Savi. Medical applications of shape memory alloys. 36(6): 683–691, 2003. ISSN 0100879X.
- D. Mandru, I. Lungu, S. Noveanu, and O. Tatar. Shape memory alloy wires as actuators for a minirobot. 1:333–336, 2010.
- E. Mathematics, K. A. Publishers, and I. M. Systems. A multi-dimensional constitutive model for shape memory alloys. pages 429–443, 1992.
- S. Maya. An experimental study on the effect of anchor diameter on the behavior of steel plate-anchor assembly embedded in concrete under biaxial loading. M.tech thesis, Indian Institute of Technology Kanpur, November 2008.
- L. McDonald Schetky. Shape memory alloy applications in space systems. 12(1):29–32, 1991. ISSN 02613069.
- J. Mohd, M. Leary, A. Subic, and M. A. Gibson. A review of shape memory alloy research , applications and opportunities. 56:1078–1113, 2014.
- J. B. I. Nemat-nasser, Wei-guo Guo. High Strain-Rate and Small Strain Response of a NiTi Shape. 127:83–89, 2005.
- S. Nemat-nasser, J.-y. Choi, W.-g. Guo, and J. B. Isaacs. Very high strain-rate response of a NiTi shape-memory alloy. 37:287–298, 2005.
- S. Nemat-Nasser, Y. Su, W. G. Guo, and J. Isaacs. Experimental characterization and micromechanical modeling of superelastic response of a porous NiTi shape-memory alloy. 53(10):2320–2346, 2005. ISSN 00225096.
- A. J. Neurohr and D. C. Dunand. Mechanical anisotropy of shape-memory NiTi with two-dimensional networks of micro-channels. 59:4616–4630, 2011.

- A. Olander. An electrochemical investigatio of solid cadmium-gold alloys. *Journal of American Chemical Society*, 54(1906):3819–3833, 1932. ISSN 0002-7863.
- M. Panico and L. C. Brinson. A three-dimensional phenomenological model for martensite reorientation in shape memory alloys. 55:2491–2511, 2007.
- M. Panico and L. C. Brinson. Computational modeling of porous shape memory alloys. 45(21):5613–5626, 2008. ISSN 00207683.
- L. Petrini and F. Migliavacca. Biomedical Applications of Shape Memory Alloys. 2011 (Figure 1):1–15, 2011. ISSN 1687-9465.
- P. Popov and D. C. Lagoudas. A 3-D constitutive model for shape memory alloys incorporating pseudoelasticity and detwinning of self-accommodated martensite. 23:1679–1720, 2007.
- M. A. Qidwai and D. C. Lagoudas. Numerical implementation of a shape memory alloy thermomechanical constitutive model using return mapping algorithms. (December 1998):1123–1168, 2000.
- L. Rimassa, M. Zoppi, and R. Molfino. A modular serpentine rescue robot with climbing ability. 36:370–376, 2009. ISSN 0143-991X.
- C. H. Ronny Pfeifera, Christian W. Müllerb. Adaptable Orthopedic Shape Memory Implants. 5:253–258, 2013.
- D. K. Sahu. Experimental study on the behavior of steel plate-anchor assembly embedded in concrete under cyclic loading. M.tech thesis, Indian Institute of Technology Kanpur, August 2004.
- M. A. Savi. Nonlinear dynamics and chaos in shape memory alloy systems. 70:2–19, 2015. ISSN 00207462.
- V. Sepe and S. Marfia. Response of porous SMA: a micromechanical study. 29:85–95, 2014.
- M. Shariyat and A. Niknami. Impact analysis of strain-rate-dependent composite plates with SMA wires in thermal environments: Proposing refined coupled thermoelasticity, constitutive, and contact models. 136:191–203, 2016. ISSN 02638223.
- J. A. Shaw and S. Kyriakides. THERMOMECHANICAL ASPECTS OF NiTi. 43(8):1243–1281, 1995.

- R. S.J. Simske and T. Bateman. Porous Materials for Bone Engineering. 250(JANUARY): 151–182, 1997. ISSN 1662-9752.
- N. N. Son and H. P. H. Anh. Adaptive displacement online control of shape memory alloys actuator based on neural networks and hybrid differential evolution algorithm. 166:464–474, 2015. ISSN 18728286.
- B. Song, W. Chen, Y. Ge, and T. Weerasooriya. Dynamic and quasi-static compressive response of porcine muscle. 40:2999–3005, 2007.
- C. Song. History and current situation of shape memory alloys devices for minimally invasive surgery. 2(1):24–31, 2010. ISSN 1875-1814.
- V. Sonkar. An experimental study on the behaviour of steel plate-anchor assembly embedded in concrete under constant compressive axial load and cyclic shear. M.tech thesis, Indian Institute of Technology Kanpur, September 2007.
- M. Sreekumar, T. Nagarajan, M. Singaperumal, M. Zoppi, and R. Molfino. Critical review of current trends in shape memory alloy actuators for intelligent robots. 34(4):285–294, 2007. ISSN 0143-991X.
- D. Starosvetsky and I. Gotman. Corrosion behavior of titanium nitride coated Ni-Ti shape memory surgical alloy. 22(13):1853–1859, 2001. ISSN 01429612.
- D. Stoeckel. Shape memory actuators for automotive applications. 11(6):302–307, 1990. ISSN 02613069.
- D. P. Thambiratnam and P. Paramasivam. Base plates under axial loads and moments. *Journal of Structural Engineering*, 112(5):1166–1181, 1986.
- H. Tobushi. Influence of strain rate on superelastic properties of TiNi shape memory alloy. 30:141–150, 1998.
- S. M. V Sepe, F Aurichhio and A. Sacco. Micromechanical analysis of porous SMA. 24, 2015.
- L. Vernon and H. Vernon. Producing molded articles such as dentures from thermoplastic synthetic resins. *US Pat*, 1941.
- J. V. G. W. J. Buehler and R. C. Wiley. Effect of Low-Temperature Phase Changes on the Mechanical Properties of Alloys near Composition TiNi. 34(5):1475–1477, 1963. ISSN 00218979.

- D. Yang. Shape memory alloy and smart hybrid composites are advanced materials for the 21st Century. pages 503–505, 2000.
- C. Yu, G. Kang, and Q. Kan. A physical mechanism based constitutive model for temperature-dependent transformation ratchetting of NiTi shape memory alloy: One-dimensional model. 78, 2014. ISSN 01676636.
- Y. Zhao and M. Taya. Analytical Modeling for Stress-Strain Curve of a Porous NiTi. 74 (2):291, 2007. ISSN 00218936.
- Y. Zhao, M. Taya, and H. Izui. Study on energy absorbing composite structure made of concentric NiTi spring and porous NiTi. 43(9):2497–2512, 2006. ISSN 00207683.